Journal of Applied Polymer Science

Controlled release of protein from magnetite–chitosan nanoparticles exposed to an alternating magnetic field

Dariush Honarmand,[1] Seyyed M. Ghoreishi,[1] Neda Habibi,[2] Ehsan Tayerani Nicknejad[1]
[1]Department of Chemical Engineering, Isfahan University of Technology, 84156-83111, Isfahan, Iran
[2]Nanotechnology and Advanced Materials Institute, Isfahan University of Technology, 84156-83111, Isfahan, Iran
Correspondence to: S. M. Ghoreishi (E-mail: ghoreshi@cc.iut.ac.ir)

ABSTRACT: In this research, the controlled release of proteins from magnetite (Fe_3O_4)–chitosan (CS) nanoparticles exposed to an alternating magnetic field is reported. Fe_3O_4–CS nanoparticles were synthesized with sodium tripolyphosphate (TPP) molecules as a crosslinking reagent. Bovine serum albumin (BSA) was used as a model protein, and its controlled release studied through the variation of the frequency of an alternating magnetic field. The results show the successful coating of CS and BSA on the Fe_3O_4 nanoparticles with an average diameter of 50 nm. Intermolecular interactions of TPP with CS and BSA were confirmed by Fourier transform infrared spectroscopy. The application of low-frequency alternating magnetic fields to such magnetic CS nanoparticles enhanced the protein release properties, in which the external magnetic fields could switch on the unloading of these nanoparticles. We concluded that enhanced BSA release from nanoparticles exposed to an alternating magnetic field is a promising method for achieving both the targeted delivery and controlled release of proteins. © 2015 Wiley Periodicals, Inc. J. Appl. Polym. Sci. **2016**, *133*, 43335.

KEYWORDS: composites; drug delivery systems; magnetism and magnetic properties

Received 29 April 2015; accepted 12 December 2015
DOI: 10.1002/app.43335

INTRODUCTION

Magnetite (Fe_3O_4) is an important kind of magnetic material; it has a cubic inverse spinal structure, which has attracted increasing attention because of its wide use in biomedical applications, such as magnetic resonance imaging,[1–5] bioseparation,[6–9] drug targeting,[10–12] and hyperthermia.[13–15] With these nanoparticles for switches, the permeability and release of proteins encapsulated in biodegradable polymeric matrices are novel approaches for the sustained and controlled release of therapeutic molecules.[11,12] It is generally recognized that when proteins are encapsulated in biodegradable polymeric matrices, their release takes place by several mechanisms, including protein desorption from the particles surface, diffusion and reabsorption of the protein through the pores of the polymer network, and degradation and erosion of the polymeric network.[13–17] Protein release from polymeric based nanoparticle–nanohydrogel systems is typified by an initial rapid release (burst effect), where 30–70% of the protein is released within the first 3–6 h, followed by a slower and much reduced further release that lasts for a few days.[18] However, these procedures take place in an uncontrolled manner, and therefore, there is a major requirement for methods that allow a desired amount of drug release in an appropriate time and position. One promising way to achieve permeability control is to embed superparamagnetic nanoparticles into a polymeric matrix. When Fe_3O_4 nanoparticles are embedded in a drug-carrier systems through the application of an external oscillating magnetic field, the carrier is modulated to release its substances.[11,12] The frequency of our experiment was 100 Hz; this was much lower than the frequency used for hyperthermia (50–100 KHz). The magnetic field was on for 200 min. We measured the temperature and did not observe any increase in the temperature; it was 37°C during the entire process. Because the temperature was not changed, protein denaturation was not expected. This was confirmed by the fact that protein denaturation occurs at 60°C. Targeted delivery was also realized by the driving of the particles by the external magnetic field. All of these applications require the use of stable Fe_3O_4 nanoparticles and the possibility of efficiently introducing functional molecules, such as proteins, to the outer surface of the Fe_3O_4 nanoparticles.[13] In this respect, the coating of a polymeric layer has been proven to be effective in the prevention of unexpected aggregation and the improvement of the chemical stability of the composite system. Chitosan (CS), a naturally occurring polymer, has been extensively researched in recent years as a primary material in the formation of carriers for therapeutic protein molecules and as nonviral gene-carrying vectors.[19–25] CS has been widely used in pharmaceutical and medical areas because of its favorable biological properties, including its biodegradability, biocompatibility, and low

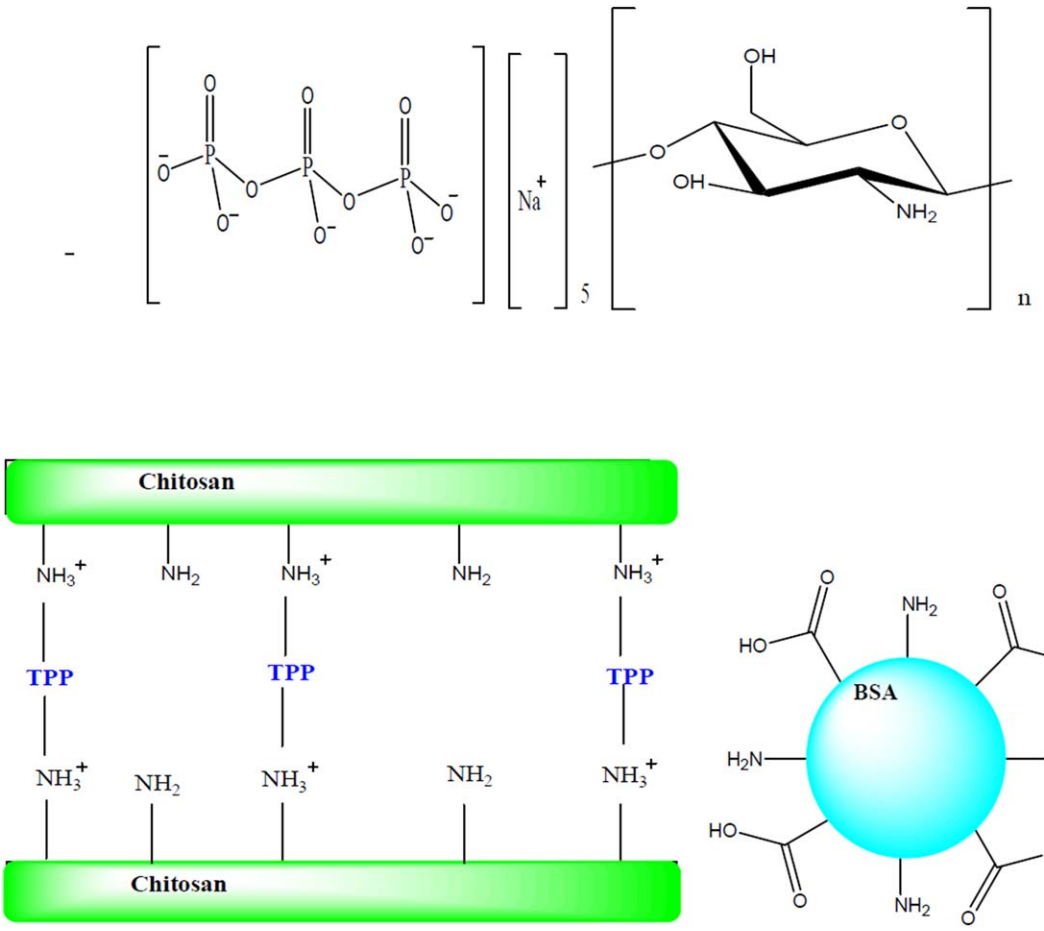

Figure 1. Chemical structures of (a) TPP, (b) CS, and (c) BSA and (d) schematic of CS crosslinked to TPP. [Color figure can be viewed in the online issue, which is available at wileyonlinelibrary.com.]

toxicity.[21] The deacetylated CS backbone of glucosamine units has a high density of amine groups; this permits electrostatic interactions with proteins and genes that carry an overall negative charge under neutral pH conditions.[25–32] To introduce a fine layer of CS on Fe_3O_4 nanoparticles, sodium tripolyphosphate (TPP) was used as a crosslinking molecule to prepare magnetic Fe_3O_4–CS nanoparticles and also to allow the attachment of other molecules on the CS layers.[33–37]

In this study, the controlled release of proteins from Fe_3O_4–CS nanoparticles exposed to an alternating magnetic field was examined. The Fe_3O_4 nanoparticles were synthesized and subsequently coated with TPP as a crosslinking reagent. The amine groups of CS solution were used to coat and crosslink with the anionic groups of TPP absorbed on the surface of the Fe_3O_4 nanoparticles. This modification first increased the chemical stability of the Fe_3O_4 nanoparticles and prevented aggregation; second, it improved the biocompatibility of the nanoparticles; and, finally, it allowed the attachment of other molecules on the Fe_3O_4 nanoparticles through crosslinking between the CS and TPP functional groups. Bovine serum albumin (BSA) as a protein model was linked to the core–shell structure of the Fe_3O_4–CS nanoparticles.[38–40] To the best of our knowledge, no data has been released on the effects of an alternating magnetic field in the controlled release of proteins. Figure 1 shows the chemical structures of TPP, CS, and BSA and a schematic of CS crosslinked to TPP. The particles were characterized by Fourier transform infrared (FTIR) spectroscopy, field emission scanning electron microscopy (FESEM), vibrating sample magnetization (VSM), and Bradford assay. CS–Fe_3O_4 nanocomposites were exposed to an alternating magnetic field, and the release of BSA was investigated by a Bradford assay for 3 h and compared to uncontrolled release at room temperature. The results first show the successful preparation of Fe_3O_4 nanoparticles coated with CS and BSA. The application of a low-frequency alternating magnetic field to such magnetic CS nanoparticles resulted in an increase in their release properties. Therefore, the external magnetic fields could switch on the unloading of these nanoparticles. Moreover, because of the enhanced BSA release from nanoparticles exposed to the alternating magnetic field, we concluded that this approach is a promising procedure for achieving both the targeted delivery and controlled release of proteins.

EXPERIMENTAL

Materials

Iron(III) chloride hexahydrate ($FeCl_3{\cdot}6H_2O$), iron(II) sulfate heptahydrate ($FeSO_4{\cdot}7H_2O$), and aqueous ammonia (28%) were purchased from Merck Co. CS (medium molecular weight),

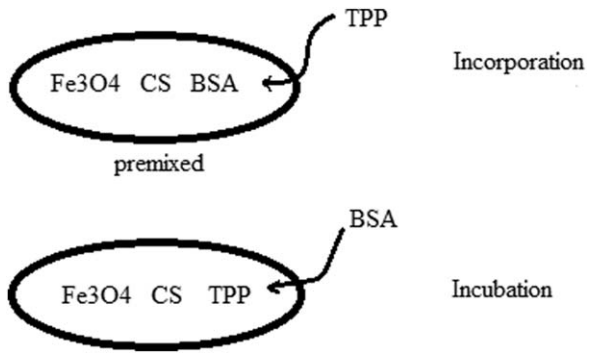

Figure 2. Schematic illustration of magnetic nanoparticle formation in incorporation and incubation methods.

acetic acid (98%), phosphate-buffered saline (PBS), TPP, and BSA were purchased from Sigma-Aldrich.

Synthesis of the Fe_3O_4 Nanoparticles

The Fe_3O_4 nanoparticles were prepared by the chemical coprecipitation route. Iron(II) chloride tetrahydrate ($FeCl_2{\cdot}4H_2O$) and $FeCl_3{\cdot}6H_2O$ were used as precursors. In a typical procedure, 2.7 g of $FeCl_3{\cdot}6H_2O$ and 1 g of $FeCl_2{\cdot}4H_2O$ were dissolved into 25 mL of 2*M* hydrochloric acid in a three-necked flask at 60°C. Then, 20 mL of ammonium hydroxide (28%) was added dropwise into the iron solution under sonication and agitation for 40 min to ensure homogeneous mixing. The pH was set to 9–11. Nitrogen was imported during the synthesis to extrude the air and prevent the oxidization of ferrous ions. After 1 h of stirring, the black precipitate of the Fe_3O_4 nanoparticles was collected by a permanent magnet, washed two times, and dried in oven for 12 h.[41–44]

Modification of the Fe_3O_4 Nanoparticles with TPP and Preparation of the Fe_3O_4–CS–TPP Nanoparticles

An amount of 10 mg of Fe_3O_4 was dissolved in 20 mL of deionized water (500 ppm), after which 3 mg of TTP was added and stirred for 30 min to form an adsorption layer around Fe_3O_4. A concentration of 2.5% w/v of CS solution was prepared by the dissolution of 0.01 g of CS powder in a 1% acetic acid solution, and this was added to the previous solution to crosslink with TPP. After 30 min of stirring, the particles were centrifuged to remove excess TPP and washed twice with distilled water. Finally, the prepared nanoparticles were suspended in water and stored at 4°C.[45–47]

BSA Loading on the Fe_3O_4–CS–TPP Nanoparticles

For the preparation of the Fe_3O_4–CS–TPP–BSA nanoparticles crosslinked with TPP, two methods, namely, incorporation and incubation, were used

In the incorporation method, BSA, Fe_3O_4, and CS were premixed in reaction systems, and then, TPP was added to start the crosslinking interactions and the formation of the Fe_3O_4–CS–TPP–BSA nanoparticles. Therefore, in this method, BSA was loaded spontaneously during the synthesis of the Fe_3O_4–CS–TPP nanoparticles. To this aim, 0.5 mg/mL Fe_3O_4, 1 mg/mL BSA, and 3 mg/mL CS dissolved in acetic acid were added, and the pH was adjusted to 5.5. An amount of 3 mg of TPP was then added to start the formation of nanoparticles, and the mixed solutions were stirred gently for 60 min. In this method, protein molecules were embedded in the CS nanomatrix, and some protein molecules were also absorbed onto its surface.[25]

In the incubation method, first, Fe_3O_4–CS–TPP nanoparticles were formed, and then, BSA was added to the reaction systems. To this aim, 30 mg of CS was dissolved in 10 mL of a 1% acetic acid solution (3 mg/mL) at pH 5.5 and stirred for 10 min. The solution was then mixed with 0.5 mg/mL Fe_3O_4 and 3 mg of TPP and stirred gently for 1 h at 25°C to allow the formation of the Fe_3O_4–CS–TPP nanoparticles. Subsequently, the obtained solution was mixed with a solution containing 1 mg/mL BSA. The nanoparticles were stirred gently for 1 h at ambient temperature to allow protein adsorption onto the magnetic nanoparticles. Fe_3O_4–BSA-loaded CS nanoparticles were formed at selected CS-to-TPP mass ratios of 3:1, 5:1, 7:1, and 9:1. Modified magnetic particles were collected by an external magnetic force, washed two times, and then stored at 4°C before they were subjected to the next application and analysis (Figure 2).

Characterization of the Nanoparticles

FTIR Spectroscopy. FTIR spectroscopy (Tensor 27, Bruker, Inc.) was used to confirm the modification of the Fe_3O_4 nanoparticles with TTP and the crosslinking of CS and BSA on the surface of the nanoparticles. For this purpose, the particles were centrifuged and washed. The water was removed, and the particles were left at room temperature and dried.

FESEM. The morphological characteristics of the nanoparticles were examined by FESEM. The FESEM micrographs of the nanoparticles were obtained with an FESEM instrument (Hitachi, model S-4160).

Bradford Assay. Bradford reagent was used to determine the concentration of the proteins in solution on the basis of the formation of a complex between a dye, Brilliant Blue G, and the proteins in solution. The protein–dye complex had a maximum absorption at 595 nm. The Bradford reagent used in this study had a high sensitivity and was able to detect protein molecules at a low concentration of 0.02 mg/mL. The linear concentration ranges were 10–100 and 100–1000 μg/mL protein, with BSA as the standard protein molecule.

VSM. The magnetic properties were analyzed with a VSM instrument (Kavir Kashan Co.). The Fe_3O_4 nanoparticles were exposed to an alternating magnetic field, and parameters such as the specific saturation magnetization, coercive force, and remanence were evaluated.

Evaluation of the Protein Encapsulation and Release

BSA-loaded CS–TPP nanoparticles were carefully transferred to a 5-mL centrifuge tube after protein loading. The nanoparticles were separated from the solution by centrifugation (16,000 rpm) at 10°C for 30 min and were suspended in 1 mL of water. To evaluate the protein encapsulation into particles, the protein content in the Fe_3O_4–TPP–CS nanoparticles was analyzed with a UV spectrophotometer at 595 nm with a Bradford protein assay. Triplicate samples were used in each analysis. The protein encapsulation efficiency (EE) was calculated with the following equation:

$$EE = \frac{(\text{Total amount of BSA} - \text{Free amount of BSA in the supernatant})}{\text{Total amount of BSA}} \times 100 \quad (1)$$

For the protein release studies, the nanoparticles in the form of sediment remaining in the centrifuge tube were transferred to a clean 5-mL centrifuge tube with 1 mL of PBS (pH 7.4). At specified collection times, the samples in the 5-mL tube were replenished with 1 mL of fresh PBS solution at $37 \pm 1°C$. Samples with a volume of 100 µl were taken from the tube, and the protein concentration was measured with Bradford reagent. Triplicate samples were analyzed. The total released bovine serum albumin mass at time i (M_i) was calculated with eq. (2):

$$M_i = C_i V + \sum (C_{i-1} V_s) \quad (2)$$

where C_i is the concentration of bovine serum albumin in the release solution at time i, V is the total volume of release solution, and V_s is volume of the sample.

To evaluate the controlled release of proteins from Fe_3O_4–TPP–CS, the particles were exposed to an alternating electromagnetic field with frequencies of 120 and 280 Hz, and a magnetic induction of 1000 Oe was applied to oscillate and disturb the Fe_3O_4 nanoparticles. The experiments were carried out with a custom-designed alternating magnetic field generator. The designed instrument (MG12) was capable of producing a magnetic field strength from 0 to 2000 Oe. The frequency of the magnetic field could be adjusted from 10 Hz to 2 kHz. The amplitude and frequency tuning was accomplished with two dials. The magnetic field was produced with an air-gapped ferrite core. The air gap was 2 mm wide, and it covered an area of $1 \times 0.5\ cm^2$. This means that the produced magnetic field was concentered onto a $0.5 \times 2\ cm^2$ area. The provided 2-mm gap could apply a magnetic field to both coated sheets and liquid suspensions. In the liquid case, a sachet was used to place the liquid in the 2-mm space. Magnetic coated nanoparticles suspended in 1 mL of PBS (pH = 7.4) were placed in a sealed plastic bag and placed in the center of the magnetic field (Figure 3). The magnetic field was on for 200 min, and at 30-min intervals, samples were taken for protein analysis. The release of BSA was subsequently measured by Bradford assay and compared to that of the control nanoparticles.

Figure 3. Instrument for producing an alternating magnetic field (MG12). [Color figure can be viewed in the online issue, which is available at wileyonlinelibrary.com.]

RESULTS AND DISCUSSION

The coating of Fe_3O_4 nanoparticles with a suitable polymer is crucial in defining its properties for biomedical applications.[48] The coating layer should be biocompatible, and it should also not cause significant changes in the magnetic properties of the nanoparticles embedded inside. The sizes of the nanoparticles are affected by several factors, including the type of polymer and the applied coating method. On the one hand, the coverage will increase the nanoparticle size, and on the other hand, it can prevent aggregation by reducing the electrostatic interactions and preventing a size increase. Moreover, the magnetic properties are decreased after a layer is coated onto Fe_3O_4 nanoparticles. Therefore, it was critical to coat a fine layer of CS on the Fe_3O_4 nanoparticles. TPP acted as a crosslinker between the functional groups of CS and BSA with Fe_3O_4 and played a pivotal role in establishing the link between these materials.[33] The pH was set to 5.5 to achieve maximum electrostatic interactions between CS and BSA.

In this study, two methods, namely, incorporation and incubation, were used to prepare the Fe_3O_4–CS–BSA nanoparticles.[26] In the incorporation method, BSA was loaded spontaneously during the synthesis of the Fe_3O_4–CS–TPP nanoparticles. The second method included BSA absorption on premade Fe_3O_4–CS–TPP nanoparticles. FESEM images of the Fe_3O_4–TPP–CS and Fe_3O_4–TPP–CS–BSA synthesized via the incubation and incorporation methods are shown in Figure 4(a–c), respectively. The size of Fe_3O_4–TPP–CS was shown to be 30 nm. After coating with BSA, the sizes changed to 46 and 51 nm for the incorporation and incubation method, respectively. The thickness of the BSA layer was found to be 12–16 nm. The results indicate that the size of the particles obtained by the incorporation method [Figure 4(c)] was lower than the particle size obtained via the incubation method [Figure 4(b)]. By measuring the BSA with a Bradford assay, we concluded that the loading capacity of the Fe_3O_4–CS–TPP nanoparticles for BSA in the incorporation method was higher; with this method, 50% BSA (1 mg/mL) was absorbed on 3 mg of the Fe_3O_4 nanoparticles after 30 min (0.5 mg/3 mg).

During the incorporation method, because BSA was loaded during the synthesis of the Fe_3O_4–TPP–CS nanoparticles, a fine layer was formed around the magnetic particles, and therefore, they appeared smaller. However, a higher amount of BSA was trapped within the matrix. During the incubation method, BSA was absorbed mostly on the surface of the Fe_3O_4–CS–TPP nanoparticles, and because BSA was a large three-dimensional protein, larger nanoparticles were formed. However, because the loading took place only on the surface and via electrostatic interactions, a lower amount of BSA was absorbed.

To determine the functional groups in the synthesized materials and to confirm the successful coating of the Fe_3O_4

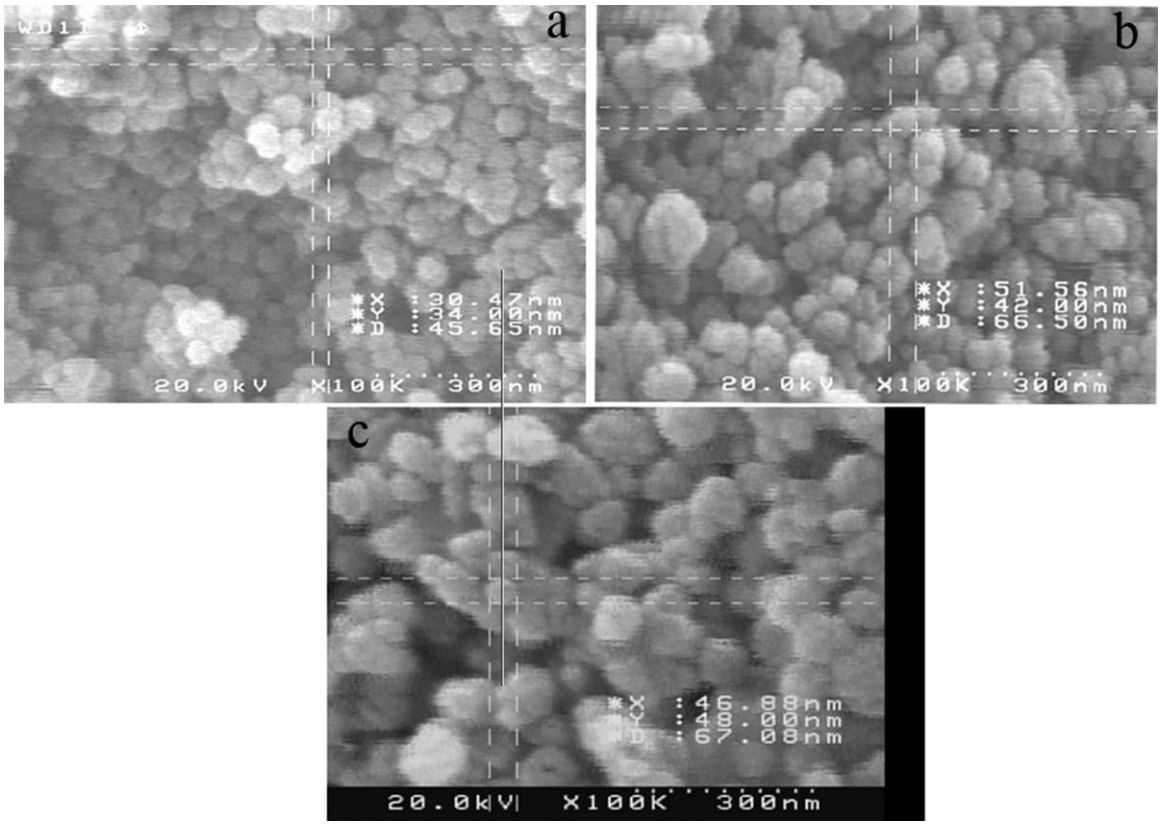

Figure 4. FESEM images of (a) Fe_3O_4–TPP–CS, (b) Fe_3O_4–TPP–CS–BSA synthesized via incubation, and (c) Fe_3O_4–TPP–CS–BSA synthesized via incorporation.

nanoparticles, an IR spectrometer was used. Figure 5(a–d) shows the FTIR spectra of Fe_3O_4, CS, BSA, and Fe_3O_4–CS–BSA nanoparticles, respectively. The peak bands at 1638, 1423, 3400, and 2800 cm^{-1} were attributed to the amide group of CS, which was observed in the CS and Fe_3O_4–TPP–CS–BSA sample. The peaks at 1380, 1500, 1680, 2900, and 3400 cm^{-1} were correlated to the amide groups of BSA. In samples containing Fe_3O_4, the absorption at 585 cm^{-1} was assigned to Fe—O vibrations. For TPP, absorptions occurred around 1230 and 1140 cm^{-1}.

The magnetic properties of the nanoparticles of Fe_3O_4, Fe_3O_4–TPP–CS, and Fe_3O_4–TPP–CS–BSA were measured through the variation of the external magnetic field (Figure 6). As shown in Figure 6, the coating of the Fe_3O_4 nanoparticles decreased the specific saturation magnetization, as the saturation magnetization of the Fe_3O_4 nanoparticles after coating with CS and BSA

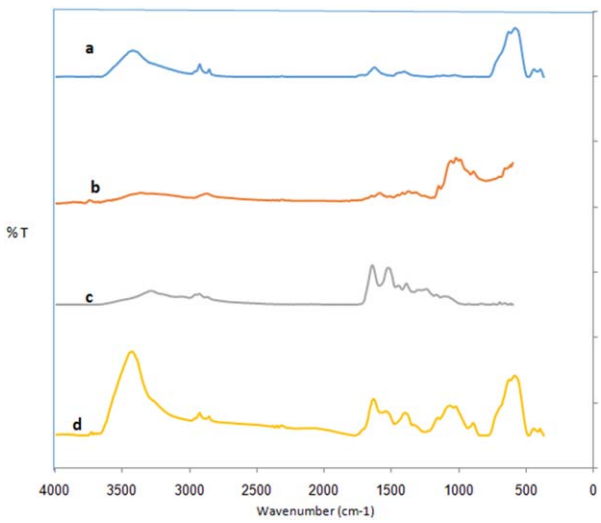

Figure 5. FTIR spectra of the (a) Fe_3O_4, (b) CS, (c) BSA, and (d) Fe_3O_4–CS–BSA nanoparticles. [Color figure can be viewed in the online issue, which is available at wileyonlinelibrary.com.]

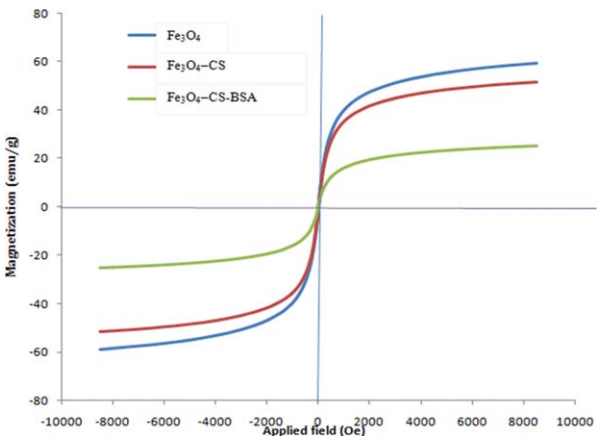

Figure 6. VSM of the Fe_3O_4, Fe_3O_4–CS, and Fe_3O_4–CS–BSA nanoparticles. [Color figure can be viewed in the online issue, which is available at wileyonlinelibrary.com.]

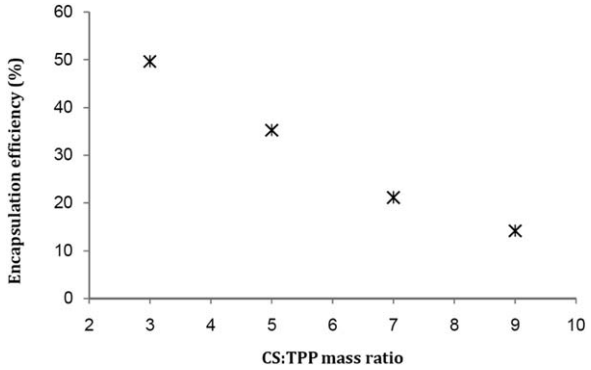

Figure 7. Effect of the CS–TPP mass ratio on the BSA EE (CS concentration = 3 mg/mL, BSA concentration = 1 mg/mL, temperature = 25°C, pH = 5.5).

went from 60 emu/g to about 53 and 32 emu/g, respectively. This was due to the fact that when the coating thickness was increased, the magnetic field was decreased. Moreover, the superparamagnetic behavior of the nanoparticles was confirmed via the obtained graphic type in Figure 6 for the Fe_3O_4, Fe_3O_4–TPP–CS, and Fe_3O_4–TPP–CS–BSA nanoparticles.

Effects of the CS–TPP Mass Ratio on the BSA Loading and Release

When the CS–TPP mass ratio was increased, the BSA uptake on the Fe_3O_4–CS nanoparticles decreased (Figure 7). This was due to the fact that the TPP molecules played an important role in establishing the binding link and uptake of BSA. When the TPP mass was reduced in the CS–TPP mass ratio at a fixed CS mass, the ability of the Fe_3O_4–CS nanoparticles to bond to the protein decreased. Moreover, a low TPP mass at a fixed CS concentration may have caused a reduction in the solution pH, with a consequential effect of a decreased overall negative surface charge carried by the protein molecules. This reduced electrostatic interactions between the positive charge of CS and the negative charge of the BSA molecules. This case emphasizes the importance of using crosslinker molecules to increase the absorption capacity and EE of biomedical drug carriers. The release properties of BSA were also studied by the variation of the CS–TPP mass ratio; this was carried out at 37°C and pH 7.4 (Figure 8). We concluded that in this case, the decrease in TPP molecules enhanced BSA release from the nanoparticles. This was explained by the fact that without the TPP molecules, BSA absorption onto the nanoparticles occurred via loose bounds and electrostatic interactions, and consequently, an easier release took place. The loading and release studies in this work proved the intermolecular interactions of the crosslinker molecules with the proteins. In drug-delivery applications, rapid and burst release from particles is undesirable because the carrier must reach its target and release its component in a slow and extended manner. In this case, the presence of TPP extended the release of BSA and prevented rapid degradation.

Effect of the Alternating Magnetic Field on BSA Release

BSA–CS–TPP–Fe_3O_4 from the incorporation method was used for further analysis because of its fine properties. To achieve the controlled magnetic release of BSA from the Fe_3O_4 nanoparticles, an oscillating magnetic field with frequencies of 120 and 280 Hz and an induction of 1000 Oe were applied to the magnetic nanoparticles. We assumed in this study that the alternating electromagnetic field influenced the Fe_3O_4 nanoparticles embedded in the CS polymer. Because the Fe_3O_4 particles were superparamagnetic, the oscillating magnetic field twisted and shook the nanoparticles at a frequency corresponding to the frequency of the applied field. This particle agitation disturbed the structure of the surrounding BSA layer, which resulted in higher BSA release. In this study, a Bradford assay was used to measure the release of BSA in the surrounding solution. To this aim, Fe_3O_4–TPP–CS–BSA nanoparticles were dispersed in PBS buffer. The nanoparticles were then placed in the center of the alternating magnetic field for 3 h. At different times, the nanoparticles were removed with an external magnetic field, the buffer was collected and substituted with fresh PBS buffer, and the BSA amount was measured with a Bradford assay. BSA release is shown in Figure 9. As shown, the samples exposed to the magnetic field showed a rapid 80% release, specifically in the first hour of exposure compared to the control sample. Without the magnetic field, in the control sample, we observed that only 30% of the absorbed BSA on Fe_3O_4–TPP–CS–BSA was released after 3 h. These results confirm the possibility of achieving the controlled magnetic release of drugs carried by Fe_3O_4 nanoparticles. The temperature was measured, and an increase in the temperature was not indicated, as the temperature was 37°C during the entire process. Because the temperature was not changed, protein denaturation was not expected. This was well

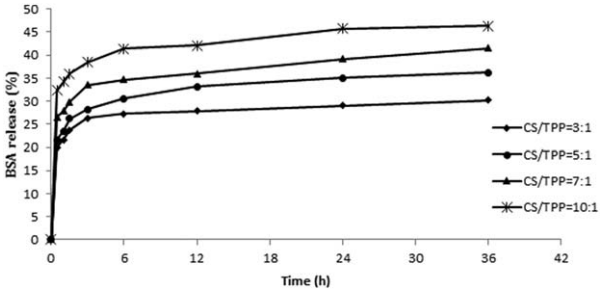

Figure 8. Effect of the CS–TPP mass ratio on the BSA release at 37°C and pH 7.4.

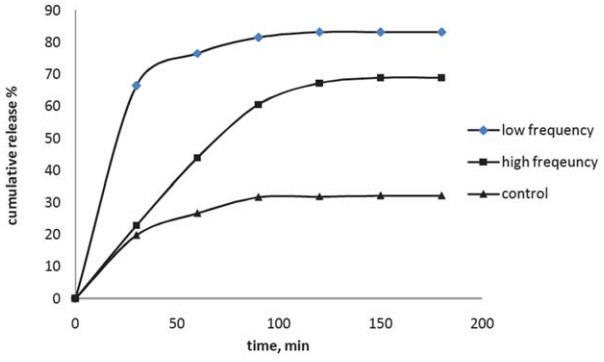

Figure 9. Schematic illustration of the Fe_3O_4–TPP–CS–BSA nanoparticles exposed to an alternating magnetic field. [Color figure can be viewed in the online issue, which is available at wileyonlinelibrary.com.]

confirmed because of the fact that protein denaturation occurred at 60°C.

The experimental data indicated that low frequencies (120 Hz) induced a higher BSA release from the Fe_3O_4–TPP–CS–BSA nanoparticles. It seemed that the increase in the frequency reduced the agitation effects of the magnetic field on the Fe_3O_4 nanoparticles; this led to a lower release of protein from the magnetic nanoparticles. This was in accordance with the fact that agitating magnetic forces were correlated with the mechanical properties of the magnetic particles, which in this case was the CS polymer embedded with BSA, and the surrounding elasticity.

First, the response of a polymer to alternating frequencies depends on the mechanical properties of the polymer itself. Polymers, including CS, are usually described as viscoelastic materials; this emphasizes their intermediate position between viscous liquids and elastic solids. An ideal elastic solid obeys Hook's law, where the stress is proportional to the strain. An ideal viscous liquid obeys Newton's law, where the stress is proportional to the rate of change in the strain. At high frequencies, a polymer may behave like a glass, with a Young's modulus of 10^9 or 10^{10} N/m^2 and will break at strains higher than 5%. At low frequencies, the polymer may behave like a rubber, with a low modulus of 10^6 or 10^7 N/m^2 and extensions larger than 100% without any permanent set. At intermediate frequencies, the polymer is neither glass nor rubber; it is viscoelastic and may dissipate a considerable amount of energy once it is strained. When we move forward form low to higher frequencies, the mechanical properties of the polymer change from viscoelastic to more glassy, and therefore, the release is decreased. In a previous study, we showed that the viscoelastic properties of a polymer highly affected its release characteristics.[40]

Saslawski *et al.*[49] studied the effect of magnetic field frequencies and repeated field applications on the release of insulin from alginates and found out that in repeated applications, an inverse effect could occur. Higher frequencies led to enhanced release in the first application; however, repeating the process for the second release application reduced the release rate because of the faster depletion of particles at these frequencies. In our experiment, the alternating magnetic field was on for 200 min; however, after 30 min intervals, the particles were taken for release measurements.[50,51]

Lu *et al.*[12] explored the use of an alternating magnetic field of 100–300 Hz and 1200 Oe to modulate the permeability of polyelectrolyte microcapsules with Co particles embedded in the matrix. Lower frequencies were shown to enhance the release rate, which is associated with the mechanical behaviors of different polymers.

Perhaps the most important reason is the resonance frequency. Resonance refers to the tendency of a system to oscillate with a greater amplitude at some frequencies than at other frequencies. Frequencies at which the response amplitude is at a relative maximum are known as resonance frequencies. At these frequencies, even small periodic driving forces can produce large-amplitude oscillations because the system stores vibrational energy. The resonance frequency is specific for each polymer and is dependent on the size and structure of the polymers.

Moreover, the induction of magnetic Fe_3O_4–TPP–CS–BSA nanoparticles with a permanent external magnetic field was studied. This was done first by the placement of a permanent magnet near the Fe_3O_4 nanoparticles in deionized water. After 5 min, all of the nanoparticles migrated to the magnet, and the bulk solution turned from a murky color to transparent. Then, similar experiments were done with Fe_3O_4–TPP–CS–BSA nanoparticles with analogous results. This showed that despite the decrease in the magnetic properties of the Fe_3O_4 nanoparticles after coating with CS and BSA, the nanoparticles could be concentrated with a permanent magnet. Therefore, we concluded that magnetic field induction provided both the accumulation of the synthesized nanoparticles to a specific location and the controlled release of their contents.

CONCLUSIONS

In this study, the controlled release of BSA from Fe_3O_4–CS nanoparticles was proposed by the application of an alternating magnetic field. Stable Fe_3O_4 nanoparticles were synthesized by coating with CS and BSA with TPP as a crosslinking molecule. The FESEM results indicated that the size of Fe_3O_4–TPP–CS was 30 nm. After coating with BSA, the size increased to 46 and 51 nm via the application of the incorporation and incubation methods, respectively. The incorporation method, in which CS and BSA were added to Fe_3O_4 during its synthesis, led to smaller nanoparticles with a higher encapsulation of BSA. This was due to the fine layer that was coated onto Fe_3O_4, and BSA was encapsulated mainly inside the matrix rather than on the surface.

The FTIR spectra confirmed the presence of functional groups of Fe_3O_4, CS, and BSA in the synthesized Fe_3O_4–CS–TPP–BSA nanoparticles and also intermolecular interactions between TPP with CS and BSA. Moreover, the superparamagnetic behavior of the nanoparticles was confirmed via VSM data. To achieve the controlled magnetic release of BSA from the Fe_3O_4 nanoparticles, an oscillating magnetic field with frequencies of 120 and 280 Hz and an induction of 1000 Oe was applied to the magnetic nanoparticles and compared to uncontrolled BSA release at 37°C. For low frequencies (120 Hz), a faster diffusion of BSA took place with higher concentrations, in which 80% BSA was released compared to the 30% BSA release of the control sample after 3 h. Therefore, the induction of an alternating magnetic field to the synthesized nanoparticles may have led to the faster and higher rate of drug release. This has important advantages for the fabrication of drug-delivery carriers.

ACKNOWLEDGMENTS

The financial support provided for this project by Isfahan University of Technology is gratefully acknowledged.

REFERENCES

1. Hao, R.; Xing, R.; Xu, Z.; Hou, Y.; Gao, S.; Sun, S. *Adv. Mater.* **2010**, *22*, 2729.
2. Bhattarai, S. R.; Bahadur, K. C. R.; Aryal, S.; Khil, M. S.; Kim, H. Y. *Carbohydr. Polym.* **2007**, *69*, 467.

3. Faraji, M.; Yamini, Y.; Rezaee, M. *J. Iran. Chem. Soc.* **2010**, *7*, 1.
4. Chang, Y.-C.; Chen, D.-H. *J. Colloid Interface Sci.* **2005**, *283*, 446.
5. He, L.; Yao, L.; Liu, F.; Qin, B.; Song, R.; Huang, W. *J. Nanosci. Nanotechnol.* **2010**, *10*, 6348.
6. Laurent, S.; Forge, D.; Port, M.; Roch, A.; Robic, C.; Vander Elst, L.; Muller, RN. *Chem. Rev.* **2008**, *108*, 2064.
7. Jain, T. K.; Richey, J.; Strand, M.; Leslie-Pelecky, D. L.; Flask, C.; Labhasetwar, V. *Biomaterials* **2008**, *29*, 4012.
8. Lu, A.-H.; Salabas, E. L.; Schüth, F. *Angew. Chem. Int. Ed.* **2007**, *46*, 1222.
9. Mody, V.; Cox, A.; Shah, S.; Singh, A.; Bevins, W.; Parihar, H. *Appl. Nanosci.* **2014**, *4*, 385.
10. Pankhurst, Q. A.; Connolly, J.; Jones, S. K.; Dobson, J. *J. Phys. D* **2003**, *36*, R167.
11. Hayashi, K.; Ono, K.; Suzuki, H.; Sawada, M.; Moriya, M.; Sakamoto, W.; Yogo, T. *ACS Appl. Mater. Interfaces* **2010**, *2*, 1903.
12. Lu, Z.; Prouty, M. D.; Guo, Z.; Golub, V. O.; Kumar, C. S. S. R.; Lvov, Y. M. *Langmuir* **2005**, *21*, 2042.
13. Jain, K. In Drug Delivery Systems; Jain, K., Ed.; Humana: New York, **2008**; p 1.
14. Shubayev, V. I.; Pisanic Ii, T. R.; Jin, S. *Adv. Drug Delivery Rev.* **2009**, *61*, 467.
15. Singh, R.; Lillard, J. W., Jr. *Exp. Mol. Pathol.* **2009**, *86*, 215.
16. Chang, K. L. B.; Lin, J. *Carbohydr. Polym.* **2000**, *43*, 163.
17. Li, Y.-P.; Pei, Y.-Y.; Zhang, X.-Y.; Gu, Z.-H.; Zhou, Z.-H.; Yuan, W.-F.; Zhou, J.-J.; Zhu, J.-H.; Gao, X.-J. *J. Controlled Release* **2001**, *71*, 203.
18. Pastorino, L.; Habibi, N.; Soumetz, F.-C.; Giulianelli, M.; Ruggiero, C. *Eur. Cells Mater.* **2011**, *22*, 66.
19. Mohammadi-Samani, S.; Miri, R.; Salmanpour, M.; Khalighian, N.; Sotoudeh, S.; Erfani, N. *Res. Pharm. Sci.* **2013**, *8*, 25.
20. Qu, J.; Liu, G.; Wang, Y.; Hong, R. *Adv. Powder Technol.* **2010**, *21*, 461.
21. Qu, J.-B.; Shao, H.-H.; Jing, G.-L.; Huang, F. *Colloids Surf. B* **2013**, *102*, 37.
22. Wu, Y.; Wang, Y.; Luo, G.; Dai, Y. *Bioresour. Technol.* **2009**, *100*, 3459.
23. Nasirimoghaddam, S.; Zeinali, S.; Sabbaghi, S. *J. Ind. Eng. Chem.* **2015**, *27*, 79.
24. Zhou, S.; Li, Y.; Cui, F.; Jia, M.; Yang, X.; Wang, Y.; Xie, L.; Zhang, Q.; Hou, Z. *Macromol. Res.* **2014**, *22*, 58.
25. Gan, Q.; Wang, T. *Colloids Surf. B* **2007**, *59*, 24.
26. Park, J. H.; Saravanakumar, G.; Kim, K.; Kwon, I. C. *Adv. Drug Delivery Rev.* **2010**, *62*, 28.
27. Amidi, M.; Mastrobattista, E.; Jiskoot, W.; Hennink, W. E. *Adv. Drug Delivery Rev.* **2010**, *62*, 59.
28. Xu, Y.; Du, Y. *Int. J. Pharm.* **2003**, *250*, 215.
29. Chen, Y.; Mohanraj, V.; Parkin, J. *Lett. Pept. Sci.* **2003**, *10*, 621.
30. Wang, J. J.; Zeng, Z. W.; Xiao, R. Z.; Xie, T.; Zhou, G. L.; Zhan, X. R.; Wang, S. L. *Int. J. Nanomed.* **2011**, *6*, 765.
31. Kafshgari, M. H.; Khorram, M.; Khodadoost, M.; Khavari, S. *Iran. Polym. J* **2011**, *20*, 445.
32. Vimal, S.; Taju, G.; Nambi, K. S. N.; Abdul Majeed, S.; Sarath Babu, V.; Ravi, M. *Aquaculture* **2012**, *358*, 14.
33. Liu, H.; Gao, C. *Polym. Adv. Technol.* **2009**, *20*, 613.
34. Mahmoudi, M.; Simchi, A.; Imani, M.; Häfeli, U. O. *J. Phys. Chem. C* **2009**, *113*, 8124.
35. Xu, Y.; Zhan, C.; Fan, L.; Wang, L.; Zheng, H. *Int. J. Pharm.* **2007**, *336*, 329.
36. Xu, Y.; Hanna, M. A. *J. Microencapsul.* **2007**, *24*, 143.
37. Ouchi, T.; Saito, T.; Kontani, T.; Ohya, Y. *Macromol. Biosci.* **2004**, *4*, 458.
38. Jiang, W.; Schwendeman, S. *Pharm. Res.* **2001**, *18*, 878.
39. Wang, Y.; Wang, X.; Luo, G.; Dai, Y. *Bioresour. Technol.* **2008**, *99*, 3881.
40. Habibi, N. *Spectrochim. Acta A* **2014**, *131*, 55.
41. Mondini, S.; Drago, C.; Ferretti, A. M.; Puglisi, A.; Ponti, A. *Nanotechnology* **2013**, *24*, 105702.
42. Sun, L.; Huang, C.; Gong, T.; Zhou, S. *Mater. Sci. Eng. C* **2010**, *30*, 583.
43. Szpak, A.; Kania, G.; Skórka, T.; Tokarz, W.; Zapotoczny, S.; Nowakowska, M. *J. Nanopart. Res.* **2013**, *15*, 1.
44. Habibi, N. *Spectrochim. Acta A* **2015**, *136*, 1450.
45. Wu, W.; He, Q.; Jiang, C. *ChemInform* **2009**, 40, i.
46. Zeng, R.; Tu, M.; Liu, H.; Zhao, J.; Zha, Z.; Zhou, C. *Carbohydr. Polym.* **2009**, *78*, 107.
47. Zhang, L.; Guo, J.; Peng, X.; Jin, Y. *J. Appl. Polym. Sci.* **2004**, *92*, 878.
48. Zhao, Q.; Li, B. *Nanomed. Nanotechnol. Biol. Med.* **2008**, *4*, 302.
49. Saslawski, O.; Weingarten, C.; Benoit, J. P.; Couvreur, P. *Life Sci.* **1988**, *42*, 1521.
50. Habibi, N.; Pastorino, L.; Ruggiero, C. *Mater. Sci. Eng.* **2014**, *35*, 15.
51. Habibi, N.; Pastorino, L.; Sandoval, O. H.; Ruggiero, C. *J. Biomater. Appl.* **2013**, *28*, 262.